

Plasmon enhanced light emission from InGaN quantum wells via coupling to chemically synthesized silver nanoparticles

John Henson,¹ John C. Heckel,² Emmanouil Dimakis,¹ Josh Abell,¹
Anirban Bhattacharyya,¹ George Chumanov,^{2,a)} Theodore D. Moustakas,¹ and
Roberto Paiella^{1,b)}

¹*Department of Electrical and Computer Engineering and Photonics Center, Boston University,
8 St. Mary's Street, Boston, Massachusetts 02215, USA*

²*Department of Chemistry and Center for Optical Materials Science and Engineering Technologies,
Clemson University, Clemson, South Carolina 29634, USA*

(Received 19 August 2009; accepted 25 September 2009; published online 15 October 2009)

Chemically synthesized single-crystal silver nanoparticles are used to demonstrate plasmon enhanced visible light emission from nitride semiconductor quantum wells. For ease of assembly and testing, the nanoparticles are embedded onto the surface of flexible resin films, which are then simply adhered on top of the light emitting samples. Large enhancements in photoluminescence efficiency are correspondingly measured at emission wavelengths near the nanoparticle plasmonic resonance. At the same time, when samples emitting at a sufficiently far detuned wavelength are used, the measured efficiency is not affected by the nanoparticles, which confirms the plasmonic origin of the observed enhancement. © 2009 American Institute of Physics.

[doi:10.1063/1.3249579]

The control of spontaneous emission by means of plasmonic interactions is currently the subject of strongly revived research interest, motivated by advances in nanofabrication technologies as well as potential applications to sensing and optoelectronic devices. Surface plasmon polaritons (SPPs) at metal surfaces and localized plasmonic resonances of metallic nanostructures can both be used to enhance the spontaneous emission rate of nearby light emitting materials,¹ by virtue of their associated large field enhancements. If suitably designed, metallic gratings and nanostructures can also effectively scatter such plasmonic excitations into radiation, thereby leading to an overall increase in light emission efficiency. Of particular importance from a technological standpoint is the use of this approach in conjunction with semiconductor optoelectronic materials,²⁻¹⁰ including InGaN/GaN quantum wells (QWs). These heterostructures can in principle cover the entire visible spectrum by tuning their alloy composition, and therefore hold great promise for several device applications including light emitting diodes. At the same time, however, their internal quantum efficiency for light emission rapidly degrades with increasing In content, leading to limited luminescence yields at longer wavelengths. Therefore, techniques for efficiency enhancement such as coupling to plasmonic excitations are especially important.

In recent years, plasmon-enhanced photoluminescence (PL) and electroluminescence (EL) have in fact been reported in InGaN/GaN QWs coated with Ag or Al films.⁴⁻⁶ In these experiments, propagating SPPs were directly excited at the semiconductor-metal interface via near-field coupling, and then partly scattered into radiation by the interface natural roughness. Correspondingly, large light emission efficiency enhancements of up to 6.8 were demonstrated.⁴ However, the use of continuous metal films offers no control of

the plasmonic resonance wavelength and extraction efficiency; furthermore the requirement of near-field proximity to the active layer makes it impractical for many device applications. These limitations can be overcome with the use of metallic nanoparticles (NPs), which can ultimately be integrated within the epitaxial material. As a first step in this direction, spontaneously formed Ag NPs fabricated via e-beam evaporation and annealing have recently been incorporated in an InGaN/GaN LED structure, resulting in an increase of the integrated PL and EL intensities by a factor of 2 and 1.3, respectively.⁷

Here we demonstrate plasmon enhanced light emission from InGaN/GaN QWs coupled to chemically synthesized single-crystal Ag NPs. These nanostructures can be fabricated in relatively dense arrays with narrow size distributions, and feature strong localized plasmonic resonances at geometrically tunable visible wavelengths with large scattering cross-sections and minimal absorption losses.^{11,12} Thus, they can provide particularly large field enhancements and efficient SPP scattering as required for plasmon enhanced light emission. For ease of assembly and testing, in the present work the NPs were embedded into flexible and optically transparent films of poly(dimethylsiloxane) (PDMS), which were further adhered to the surface of the light emitting samples. Encapsulation into PDMS has also the advantage of protecting the NPs from oxidization.

The single-crystal Ag NPs were synthesized in a round-bottom flask filled with saturated silver(I) oxide in ultrapure water at 70 °C under 0.69 bar of excess pressure of hydrogen gas. The hydrogen reducing atmosphere causes the nucleation and growth of Ag NPs, whose diameter depends on the reaction time.¹¹ The immobilization procedure of these NPs into PDMS films is described in detail elsewhere.¹³ Briefly, Ag NPs were self-assembled onto 25 × 25 mm², poly(4-vinylpyridine) (PVP) modified glass substrates and further covered with a thin layer of liquid resin (Sylgard 184 in 10:1 resin:curing agent ratio, Dow Corning

^{a)}Electronic mail: gchumak@clemson.edu.

^{b)}Electronic mail: rpaiella@bu.edu.

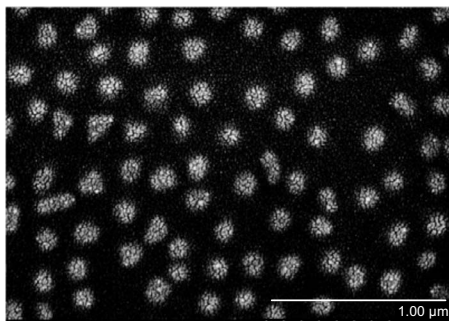


FIG. 1. Scanning electron microscopy image of Ag NPs embedded in a PDMS film.

Corp.), that was allowed to polymerize. After completion of the polymerization, the cured PDMS films were peeled off the substrates with the Ag NPs embedded on their surface.

The resulting PDMS films contain robust two-dimensional arrays of Ag NPs in an optically transparent matrix, slightly protruding out of the surface. A scanning electron microscopy image of such an array is shown in Fig. 1, illustrating the NPs size and shape uniformity. A typical UV/visible extinction spectrum of the NPs used in this work is shown in Fig. 2, where a strong resonance peak at 533 nm and a weaker shoulder near 469 nm are clearly seen. These are attributed to collective quadrupolar and octupolar plasmonic resonances of the NP array, respectively, as discussed in Ref. 14. The spectral position and strength of these resonances depend on the NPs geometry as well as mutual distance within the array. It should also be noted that, for large NPs such as the ones used in this work (having average diameter of about 200 nm), the extinction cross-section is dominated by light scattering as opposed to optical absorption.¹²

Plasmon enhanced light emission was demonstrated with samples based on two InGaN/GaN QW structures emitting near 470 nm, close to the peak of the extinction spectrum of Fig. 2. Both structures were grown by rf-plasma-assisted molecular beam epitaxy on a GaN template on *c*-plane sapphire. One structure consists of five pairs of nominally 16-Å-thick InGaN wells and 30-Å GaN barriers (structure A), while the other comprises three pairs of 40-Å InGaN wells and 50-Å GaN barriers (structure B). In both cases, the InN mole fraction in the wells is approximately 20%. To confirm the plasmonic origin of the observed enhancement, we also tested

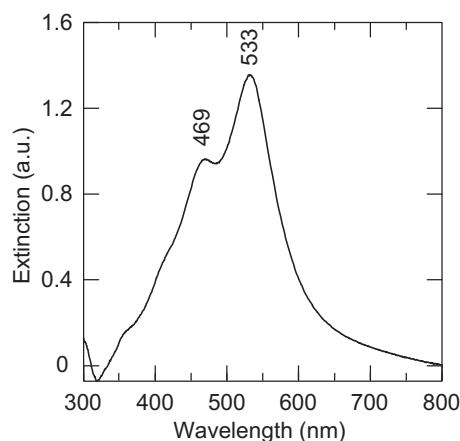


FIG. 2. Measured extinction spectrum of the Ag NPs used in this work.

samples from a third wafer (C) with emission wavelength near 350 nm, i.e., well outside of the NP extinction spectrum. The active layer of this structure consists of a single 20-Å GaN well with 100-Å $\text{Al}_{0.10}\text{Ga}_{0.90}\text{N}$ barriers, grown on an $\text{Al}_{0.30}\text{Ga}_{0.70}\text{N}$ template on *c*-plane sapphire. To ensure strong coupling between the light emitting excitons in the QWs and the NP plasmonic excitations, in all three structures no additional layer was grown over the topmost barrier so that the QWs are as close as possible to the NPs.

All samples were characterized via PL measurements, with the QW emission both photoexcited and collected through the sapphire substrates. In each experiment, two samples from the same wafer were first measured side by side, without any PDMS coating. The two samples were then coated, respectively, with a control PDMS film containing no NPs and with the NP film of Fig. 2, and again measured simultaneously. The PL spectra of the InGaN/GaN QW samples were obtained with a nitride-based diode pump laser emitting at 375 nm (between the QW emission wavelength and the absorption edge of the GaN template near 360 nm). In the case of samples from wafer C, a HeCd pump laser emitting at shorter wavelength (325 nm) was used, due to the larger bandgap energy of GaN/AlGaIn QWs. It is important to note that both pump wavelengths lie outside of the NP extinction spectrum; therefore the NPs do not produce any appreciable reflection and scattering of the transmitted pump light back into the QWs.

The measurement results are summarized in Fig. 3. The PL spectra shown in Fig. 3(a) were measured with a sample from wafer A, with no coating (dashed curve) and with the NP-free PDMS control film (solid curve). As illustrated by these data, application of the PDMS control film consistently produces a decrease in PL intensity as compared to the samples without any film. This behavior is ascribed to the reduced back reflection of the pump beam from the nitride/PDMS interface relative to the nitride/air interface, so that less pump light is absorbed in the QWs in the presence of the PDMS films. On the other hand, application of the film containing the Ag NPs leads to a strong increase in PL intensity. This is illustrated in Fig. 3(b), where the dashed and solid curves are the PL spectra of the simultaneously measured sample from wafer A, with no coating and with the NP film, respectively. Normalizing to the data of Fig. 3(a) to account for the reduction in reflected pump light from the nitride/PDMS interface, we conclude that the integrated and peak PL efficiencies of this sample were enhanced by a factor of about 4.2 and 4.0, respectively.

Similar results were obtained with all other pairs of InGaN/GaN QW samples. An example from wafer B is shown in Figs. 3(c) and 3(d), which demonstrate a normalized enhancement in peak and integrated emission efficiencies of about 2.7. These two sets of data are representative of the spread of values in the measured enhancement factors, which we mainly attribute to variable adhesion of the PDMS film, possibly related to variations in surface roughness. Finally, the results of similar measurements with samples based on the GaN/AlGaIn QW structure (wafer C) are shown in Figs. 3(e) and 3(f). In this case, the film with the Ag NPs produces a decrease in PL intensity by roughly the same amount observed with the control film. This behavior is consistent with the large detuning between the emission wavelength of these samples and the plasmon resonance of the NPs. These results therefore confirm that the light emission

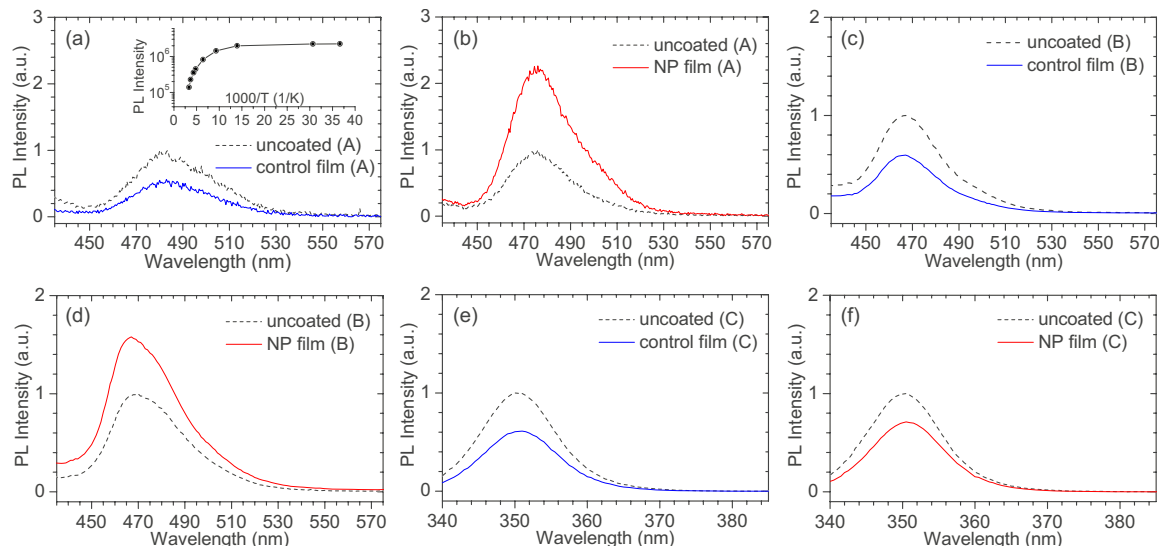


FIG. 3. (Color online) Measured PL spectra from various combinations of coated and uncoated samples. (a) Sample from wafer A, with no coating (dashed black curve) and with the NP-free PDMS control film (solid blue). (b) Sample from wafer A, with no coating (dashed black curve) and with the NP film (solid red). [(c) and (d)] same as [(a) and (b)], respectively, with a sample from wafer B. [(e) and (f)] same as [(a) and (b)], respectively, with a sample from wafer C.

efficiency enhancement measured with the InGaN/GaN samples is in fact due to the resonant coupling between the radiating excitons and the plasmonic excitations of the NPs.

The enhancement F in spontaneous emission rate due to this coupling (which is approximately equal to the average electromagnetic field-intensity enhancement in the active layer⁹) can be estimated from the measured PL efficiency ratio η'/η , where η' and η are the emission efficiencies with and without the NPs, respectively. Specifically, using the simple expressions for η and η' discussed in Ref. 15 and assuming that the density of radiation modes is not affected by the NPs, we have

$$\frac{\eta'}{\eta} = \frac{1 + (F - 1)\eta_{extr}^{SPP}/\eta_{extr}^{rad}}{1 + (F - 1)\eta_{int}}, \quad (1)$$

where η_{extr}^{rad} and η_{extr}^{SPP} are the extraction efficiencies of the emitted photons and SPPs, respectively, and η_{int} is the internal quantum efficiency of the active material. The latter parameter can be obtained from the ratio of the measured PL signals at room temperature and near 10 K.¹⁶ An Arrhenius plot of the integrated output intensity of a sample from wafer A is shown in the inset of Fig. 3(a), yielding a value of η_{int} of about 6.2%. Furthermore, we assume $\eta_{extr}^{SPP}/\eta_{extr}^{rad} \approx 1$ because of the large scattering and small absorption cross sections of the NPs used in this work.

Using Eq. (1) we then find that the PL efficiency ratio of 4.2 measured in Figs. 3(a) and 3(b) corresponds to an enhancement factor F of about 5.3. It should be emphasized that this is an average over the entire volume of the QW active layer and is limited by the density of NPs in the array. In any case, similar values were also estimated in Ref. 9, where arrays of lithographically defined Ag NPs were used to increase the PL efficiency of nearby silicon quantum dots. Even larger enhancements can be expected with arrays of higher density (e.g., using more closely packed NPs or NP

multilayers) and/or by further matching the array plasmonic resonance to the emission spectrum. If properly integrated within the active region of a full LED structure, e.g., as in the work of Ref. 7, these nanostructures are therefore promising for the development of high-efficiency solid-state light sources.

This work was supported by the Department of Energy under Grant Nos. DE-FG02-06ER46332 and DE-FG02-06ER46342.

- ¹W. L. Barnes, *J. Mod. Opt.* **45**, 661 (1998).
- ²I. Gontijo, M. Boroditsky, E. Yablonovitch, S. Keller, U. K. Mishra, and S. P. DenBaars, *Phys. Rev. B* **60**, 11564 (1999).
- ³A. Neogi, C.-W. Lee, H. O. Everitt, T. Kuroda, A. Tackeuchi, and E. Yablonovitch, *Phys. Rev. B* **66**, 153305 (2002).
- ⁴K. Okamoto, I. Niki, A. Shvartsner, Y. Narukawa, T. Mukai, and A. Scherer, *Nature Mater.* **3**, 601 (2004).
- ⁵Y. C. Lu, C. Y. Chen, D. M. Yeh, C. F. Huang, T. Y. Tang, J. J. Huang, and C. C. Yang, *Appl. Phys. Lett.* **90**, 193103 (2007).
- ⁶D. M. Yeh, C. F. Huang, C. Y. Chen, Y. C. Lu, and C. C. Yang, *Appl. Phys. Lett.* **91**, 171103 (2007).
- ⁷M. K. Kwon, J. Y. Kim, B. H. Kim, I. K. Park, C. Y. Cho, C. C. Byeon, and S. J. Park, *Adv. Mater.* **20**, 1253 (2008).
- ⁸C. W. Lai, J. An, and H. C. Ong, *Appl. Phys. Lett.* **86**, 251105 (2005).
- ⁹J. S. Biteen, L. A. Sweatlock, H. Mertens, N. S. Lewis, A. Polman, and H. A. Atwater, *J. Phys. Chem. C* **111**, 13372 (2007).
- ¹⁰J. B. Khurgin, G. Sun, and R. A. Soref, *Appl. Phys. Lett.* **93**, 021120 (2008).
- ¹¹D. D. Evanoff, Jr. and G. Chumanov, *J. Phys. Chem. B* **108**, 13948 (2004).
- ¹²D. D. Evanoff, Jr. and G. Chumanov, *J. Phys. Chem. B* **108**, 13957 (2004).
- ¹³S. Malynych, H. Robuck, and G. Chumanov, *Nano Lett.* **1**, 647 (2001).
- ¹⁴S. Malynych and G. Chumanov, *J. Am. Chem. Soc.* **125**, 2896 (2003).
- ¹⁵J. Henson, A. Bhattacharyya, T. D. Moustakas, and R. Paiella, *J. Opt. Soc. Am. B* **25**, 1328 (2008).
- ¹⁶Y. Kawakami, K. Omac, A. Kaneta, K. Okamoto, T. Izumi, S. Saijou, K. Inoue, Y. Narukawa, T. Mukai, and S. Fujita, *Phys. Status Solidi A* **183**, 41 (2001).